ATLAS High-Level Trigger performance for calorimeter-based algorithms in LHC Run-I

2014 J. Phys.: Conf. Ser. 513 012022

(http://iopscience.iop.org/1742-6596/513/1/012022)

Journal of Physics: Conference Series **513** (2014) 012022 doi:10.1088/1742-6596/513/1/012022

ATLAS High-Level Trigger performance for calorimeter-based algorithms in LHC Run-I

A Mann, on behalf of the ATLAS Collaboration

Ludwig-Maximilians-Universität München, Fakultät für Physik,
Am Coulombwall 1, 85748 Garching, Germany

E-mail: mann@cern.ch

Abstract. During Run-I of the Large Hadron Collider at CERN the ATLAS detector recorded more than 26 fb^{-1} of proton-proton collision events. One of the key components of the ATLAS detector is its trigger system. In order to keep up with the fast-paced evolution of the beam conditions during Run-I, the trigger selection had to be constantly adapted. For most of the calorimeter-based triggers only modest modifications of the thresholds had to be made, given the change in instantaneous luminosity of five orders of magnitude. This was achieved by various improvements in the High-Level Trigger algorithms, in several places abandoning the original RoI-based concept and introducing new features to overcome previous limitations. The excellent performance of both ATLAS and the LHC made possible the discovery of a new particle already during Run-I, the long-sought Higgs boson.

1. Introduction

Run-I of the Large Hadron Collider (LHC) [1] comprises three data-taking periods in the years 2010 – 2012. During this time, more than 26 fb^{-1} of proton-proton collision data have been collected with the ATLAS detector [2]. The task of the ATLAS trigger and data-acquisition system (TDAQ) [3] is to reduce the initial event collision rate of up to 20 MHz during Run-I to the maximum storage rate of a few hundreds of events per second. Due to the very successful ramp-up of the instantaneous luminosity, the trigger algorithms had to be constantly adapted and improved in order to keep the rates within the limits given by the hardware constraints. The calorimeter-based triggers, selecting events with electrons, photons, taus, missing transverse energy ($E_{\text{T}}^{\text{miss}}$), or jets, are primarily based on information from the electromagnetic and hadronic calorimeters of the ATLAS detector. In addition, electron and tau triggers also use tracking information. The calorimeter-based triggers in particular had to cope with an increasing level of background activity from the increasing number of concurrent events (in-time pile-up). The present work describes the High-Level Trigger algorithms for these triggers[1], with focus on their performance and changes necessary in view of increasing in-time pile-up.

1.1. The ATLAS trigger system

The ATLAS trigger system is designed as a three-tiered system. The first level, Level 1 (L1), is hardware-based and runs on fast, custom-built electronics [5]. It uses coarse-grained information from the calorimeters and two types of fast-response muon chambers. During Run-I no track

[1] For a description of the ATLAS Level-1 calorimeter trigger cf. [4].

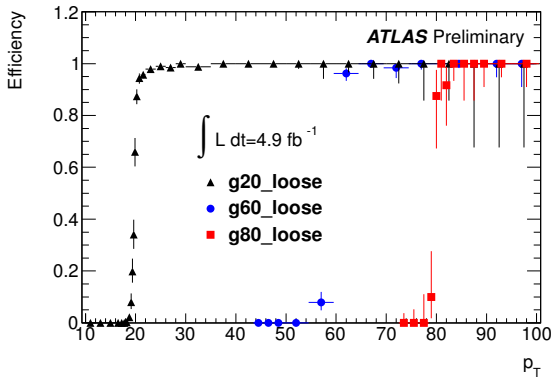

Figure 1. Efficiencies of photon triggers in 2011 relative to their respective L1 seeds as function of "tight" offline photon p_{T} [6].

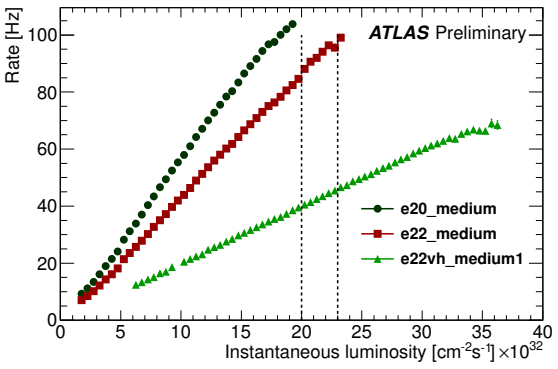

Figure 2. Single-electron trigger rates in 2011 as function of instantaneous luminosity, showing the achieved reduction [6].

reconstruction and no topological cuts were affordable at this trigger level. L1 identifies regions of interest (RoIs), geometrical regions with significant detector activity, which are then passed as seeds to the next trigger level. Level 2 (L2) is software-based and runs on a dedicated computing cluster built from commercially available hardware. It fetches data from the RoIs at full detector granularity, and adds tracking and topological information. If an event is accepted at L2, event building is initiated and the event passed to the Event Filter (EF). Like L2, the EF is software-based and runs on its own dedicated computing cluster. It employs offline-like algorithms which have access to the full event information. L2 and EF are collectively called High-Level Trigger (HLT). Table 1 shows the evolution of important figures of merit for the ATLAS TDAQ and the LHC during Run-I.

Table 1. Evolution of important figures of merit for ATLAS and the LHC during Run-I

ATLAS TDAQ working point	Design	2010	2011	2012
Peak L1 output rate (kHz)	75	20	50	70
Peak L2 output rate (kHz)	3.5	3.5	5.5	6.5
EF output rate (kHz)	0.2	0.35	0.4	0.7
RoI data fraction (%)	2	5	5	10
Integrated luminosity (recorded, 1/fb)		0.045	5.08	21.3
LHC beam conditions	**Design**	**2010**	**2011**	**2012**
Center-of-mass energy $\sqrt{s}$ (TeV)	14	7	7	8
Peak average in-time pile-up	23 (avg.)	3	18	36
Peak instantaneous luminosity (Hz/cm^2)	10^{34}	$2.07 \cdot 10^{32}$	$3.65 \cdot 10^{33}$	$7.73 \cdot 10^{33}$
Peak number of proton bunches per beam	2808	348	1331	1380
Typical bunch spacing within a train (ns)	25	150	50	50

2. Performance of calorimeter-based High-Level Trigger algorithms during Run-I

2.1. Electron and photon triggers

The electron and photon trigger chains start from common seeds at L1, where no tracking information is available. The discrimination of electrons and photons from backgrounds at the HLT is based on cuts on a set of identification variables similar to those used offline: Shower

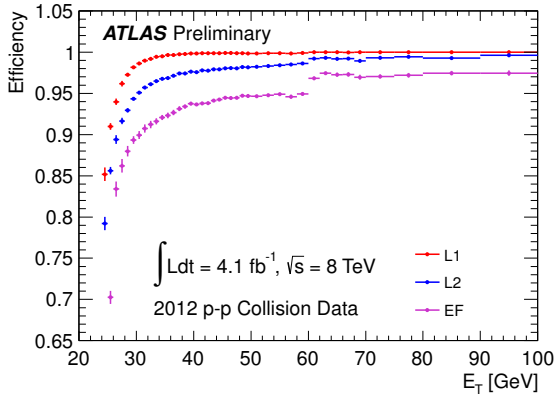

Figure 3. Efficiency of the logical OR of the two primary single-electron triggers, e24vhi_medium1 + e60_medium1, for offline electrons with $E_{\mathrm{T}} > 25\,\mathrm{GeV}$ [7].

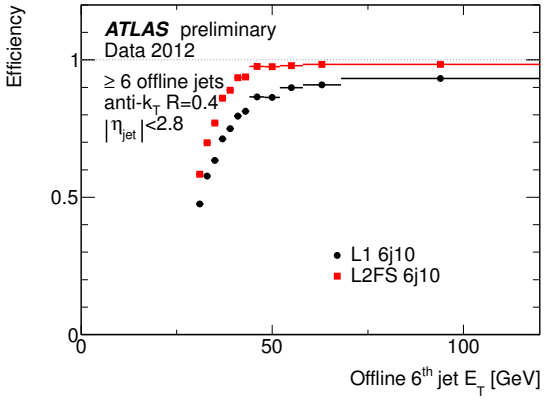

Figure 4. Efficiency of L1 and L2FS triggers in events with at least 6 offline jets with $E_{\mathrm{T}} > 30\,\mathrm{GeV}$. L2FS recovers efficiency lacking at L1 in multijet events [8].

shape information is reconstructed from fine-granularity information from the calorimeters, and in addition tracking information is used to identify electrons. In addition to the primary triggers, supplementary triggers such as J/Ψ triggers and W tag & probe triggers for low transverse momentum (p_{T}) electrons and supporting triggers for background estimates are available.

The photon triggers had a very stable performance in both 2011 and 2012. They exhibit very sharp turn-on behavior and plateau efficiencies close to 100 % as is shown in Figure 1, independent of η and in-time pile-up[2]. The EF threshold of the lowest-threshold unprescaled photon trigger chain was raised from 60 to 80 GeV in 2011 and to 120 GeV for 2012.

For the lowest-threshold unprescaled electron trigger the EF threshold was raised from 20 to 22 GeV in 2011 and to 24 GeV for 2012. Furthermore, in 2011 the electron identification criteria at L2 were brought closer to the EF level selections, and an additional selection was deployed to reconcile the trigger selection with the re-optimised offline selection for electrons with better performance under high pile-up conditions. Figure 2 shows the rate reduction achieved in 2011, where "vh" indicates a modified L1 seed [6]. In 2012 a pile-up robust track isolation was introduced and the identification cuts at the HLT were changed to improve pile-up robustness by cutting harder on pile-up insensitive quantities and looser on sensitive ones. Figure 3 shows the efficiency of the primary single-electron triggers used in 2012.

2.2. Jet triggers

Jet triggers scan for collimated energy deposits in the calorimeters arising from the hadronization of high-energy quarks or gluons. Jets are the most common final-state object at the LHC.

The original, entirely RoI-based design of the jet trigger suffered from the fact that only one jet per RoI could be reconstructed, leading to efficiency losses for events with many and near-by jets, and in general the discrepancy between trigger and offline algorithms used for jet finding. However, in 2010 the EF jet algorithms were running in pass-through mode (i. e. did not reject events). Before the activation of the EF for rejection of events at the beginning on 2011, the RoI-based algorithms at EF were replaced by a full-scan algorithm (EFFS), which finds jets independently of any L1 or L2 seed, using instead topological clusters as input to an anti-k_t algorithm. Similarly, the simplified cone algorithm at L2 was replaced in 2012 by a full scan (L2FS, also called L1.5). It consists in an unseeded fast anti-k_t algorithm [9] applied to trigger

[2] η is pseudorapidity, ϕ the angle in the transverse plane of the coordinate system used by ATLAS [2].

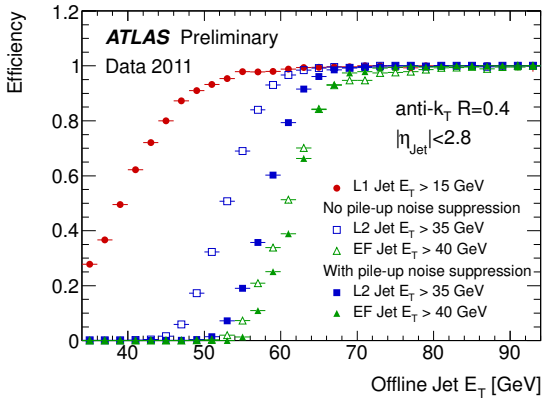

Figure 5. Comparison of the efficiency for a single jet trigger chain with and without noise suppression applied [8].

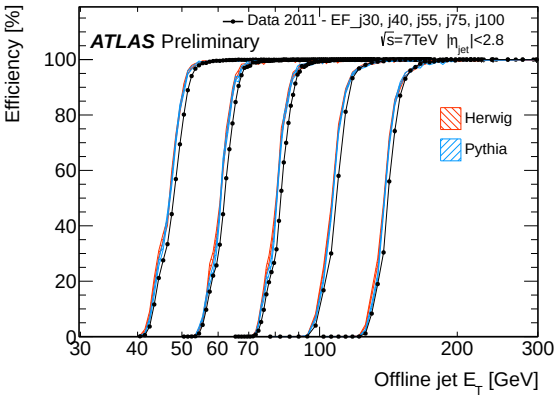

Figure 6. Efficiency for various Event Filter trigger chains calculated using the bootstrap method. [8].

towers with a granularity of $\Delta\eta \times \Delta\phi = 0.1 \times 0.1$, coarser than cell-level granularity due to time constraints. This breaks the RoI concept, but is closer to the offline selection and recovers inefficiencies for multi-jet topologies and close-by jets as can be seen in Figure 4. Starting in May 2011, two-sided configurable cuts at cell-level were introduced, taking into account measured noise from pile-up and calorimeter electronics. This leads to a significant improvement at L2 as shown in Figure 5. The overall 99 % efficiency point is lower by about 5 GeV. The effect at EF is smaller because topological clustering already includes noise suppression. Figure 6 shows the EF efficiency for single jet triggers in 2012 computed with respect to events collected by a L2 trigger at 100 % efficiency. The improvements also made possible to introduce in 2012 efficient triggers on the sum of the p_{T} of all identified jets (H_T) and on boosted topologies with wide energy deposits not well contained in single RoIs.

2.3. E_T^{miss} triggers

The $E_{\mathrm{T}}^{\mathrm{miss}}$ triggers are designed to select collision events containing particles not interacting with the detector material, identified as a significant imbalance in the vectorial sum of all particle energies transverse to the beam axis[3]. Being a global sum of energy deposits over the full calorimeter, this type of triggers are very susceptible to pile-up effects. An increase of in-time pile-up leads to an increase of the average energy deposited in the calorimeter and thus in measurement fluctuations. This causes strong non-linearities in the rates of low-threshold $E_{\mathrm{T}}^{\mathrm{miss}}$ triggers as function of luminosity as can be seen in Figure 7, and presents a challenge for these triggers. Algorithms and noise thresholds need to be carefully tuned to allow for a separation of different sources of $E_{\mathrm{T}}^{\mathrm{miss}}$: real $E_{\mathrm{T}}^{\mathrm{miss}}$ from undetectable particles and fake $E_{\mathrm{T}}^{\mathrm{miss}}$ from pile-up and resolution effects.

In 2011 the value of $E_{\mathrm{T}}^{\mathrm{miss}}$ at L2 was basically the same as that computed at L1, and thus the $E_{\mathrm{T}}^{\mathrm{miss}}$ trigger at L2 suffered from the poor resolution of the L1 measurement. A substantial improvement was achieved after an upgrade of the calorimeter readout in 2012 and the introduction of a parallel line of data access. This allowed for a fast recomputation of $E_{\mathrm{T}}^{\mathrm{miss}}$ at L2 from cell-based sums of E_{T} provided by the calorimeter front-end boards, yielding a much better resolution than the trigger-tower based $E_{\mathrm{T}}^{\mathrm{miss}}$ of L1. At EF level, the cell-based algorithm was replaced by a new algorithm summing calibrated topological clusters in 2012, which also applies

[3] Muon information is available at both L2 and EF, but was not included in the $E_{\mathrm{T}}^{\mathrm{miss}}$ computation in active 2011 triggers, and in 2012 only in one combined chain at EF level.

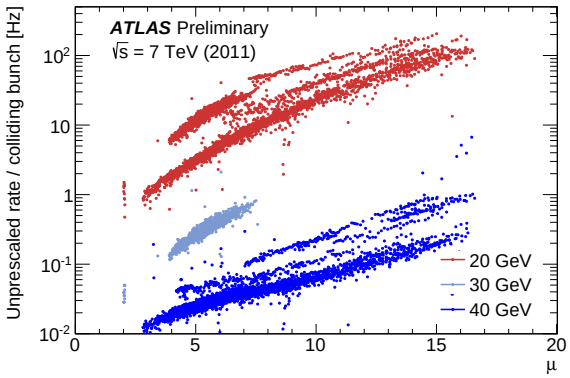

Figure 7. Rates per bunch crossing for low-threshold $E_{\mathrm{T}}^{\mathrm{miss}}$ triggers in 2011 as function of the number of concurrent interactions μ, illustrating the stronger-than-linear increase of the rates as function of in-time pile-up [11].

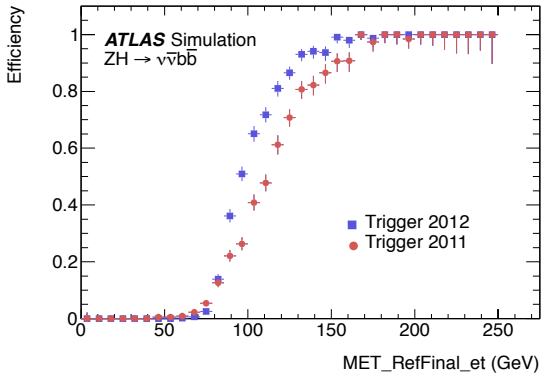

Figure 8. Efficiency of the lowest unprescaled $E_{\mathrm{T}}^{\mathrm{miss}}$ trigger chains in 2011 (thresholds: 50, 55, 60 GeV at L1, L2, EF) and 2012 (40, 45, 80 GeV, using topological clusters with local weight calibration at EF) [11].

a local-weight calibration for the cell energies [10]. Figure 8 shows a comparison of the efficiency of the lowest-$E_{\mathrm{T}}^{\mathrm{miss}}$ unprescaled triggers in 2011 and 2012 in simulated $ZH \to \nu\nu b\bar{b}$ events. Despite the harsher pile-up conditions in 2012, looser trigger requirements than in 2011 could be afforded, and the acceptance is considerably improved. Another important development in 2011 was the introduction of $E_{\mathrm{T}}^{\mathrm{miss}}$ significance (XS) triggers. They exploit the different scaling behavior of fake and real $E_{\mathrm{T}}^{\mathrm{miss}}$ with $\sum E_T$, the scalar sum of the transverse energies of all particles, and allow to recover events with real $E_{\mathrm{T}}^{\mathrm{miss}}$ below the $E_{\mathrm{T}}^{\mathrm{miss}}$ trigger thresholds.

2.4. Tau triggers

The tau triggers select hadronic decays of tau leptons, which are identified as collimated energy deposits in the calorimeters accompanied by one or a low number of matching charged tracks. Similar to the electron and photon triggers, the HLT tau algorithms accept events based on selection cuts on tracking and calorimeter-based variables, where the EF is kept as close as possible to the offline selection. The HLT tau algorithms have been run in pass-through mode until mid of 2010.

For 2011 data-taking, several aspects of the cut-based selection at L2 and EF were improved and modified to bring it closer to the offline selection: At L2 the geometrical window around the RoI was enlarged from 0.6×0.6 to 0.8×0.8, noise thresholds at cell level were introduced, and the definition of the EM radius variable, one of the selection variables, was changed to match the offline definition. At EF level, a tighter track selection and more shape variables were used. In addition shape variables were made dependent on the transverse energy of the tau candidate, and the tau energy was now computed from topological clusters at a local calibration scale [12].

A severe performance degradation in the efficiency of the tau trigger as a function of the in-time pile-up was observed in 2011, as shown in Figure 9. Several adjustments in the definition of the identification variables at L2 were thus done for 2012: The cone size used to compute the L2 EM radius, i. e. the energy-weighted shower radius of the L2 tau candidate, was reduced from 0.4 to 0.2. Additionally, only tracks with longitudinal impact parameters compatible with that of the highest-p_{T} track, $|\Delta Z_0| < 2\,\mathrm{mm}$, were used in the L2 tau identification. Also the track-based isolation was complemented by a calorimeter-based isolation cut. At EF level, the cut-based selection was replaced by a multi-variate algorithm based on boosted-decision trees (BDT) in 2012. Figure 10 shows the efficiency of a 20 GeV tau trigger for offline taus with $p_{\mathrm{T}} > 30\,\mathrm{GeV}$

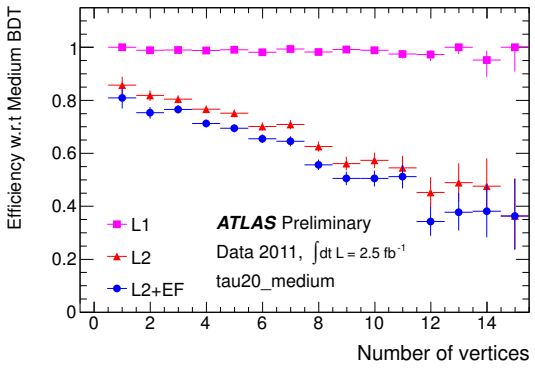

Figure 9. Efficiency of the cut-based trigger selection (tau20_medium) measured in 2011 data [13].

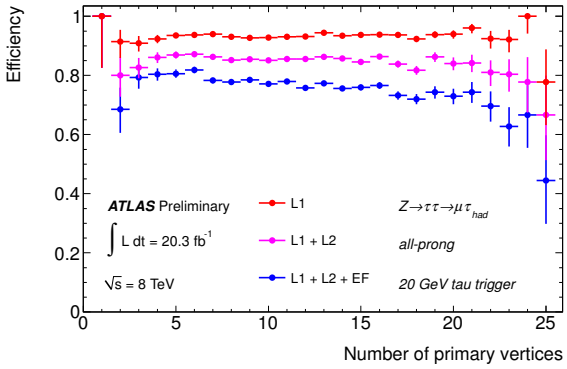

Figure 10. Efficiency of the BDT-based trigger selection measured in 2012 data for a 20 GeV tau trigger. [13].

measured in 2012 data, demonstrating the pile-up robustness achieved by the improved trigger selection at L2 and EF.

3. Ideas and prospects for Run-II

In Run-II of the LHC, foreseen for 2015 – 2018, the center-of-mass energy is expected to be raised to 13 TeV and the instantaneous luminosity to possibly exceed the design value of 10^{34} Hz/cm^2. Improvements of the ATLAS TDAQ system planned for Run-II include a new L1 Topological processor allowing to use topological cuts not only at the HLT but also at L1, and a new FastTracker, a hardware-based tracking system, which provides the HLT with track parameters for the full event and could be used to reconstruct primary vertices, giving an event-by-event estimate of pile-up. A network upgrade and new read-out systems will allow a higher data access rate, and L2, EB, and EF will be merged, yielding a unified HLT architecture [14]. The output rate of L1 will be increased from 70 to 100 kHz and the final storage rate up to 1 kHz.

The trigger strategy for Run-II will benefit from the TDAQ upgrades. Nevertheless, algorithms and calibrations will still need to become even more pile-up robust, and isolation requirements to be revisited to avoid inefficiencies. Like the tau triggers, the electron and photon triggers could switch to multi-variate algorithms. In general, all triggers will have to move to tighter selections and try to be closer to the offline selection, ensuring a versatile, efficient and unbiased set of signal and background triggers for Run-II.

References

[1] Evans L and Bryant P 2008 *JINST* **3** S08001
[2] ATLAS Collaboration 2008 *JINST* **3** S08003
[3] ATLAS Collaboration CERN-LHCC-2003-022 `http://cds.cern.ch/record/616089`
[4] Achenbach R *et al.* 2008 *JINST* **3** P03001
[5] ATLAS Collaboration CERN-LHCC-98-014 `http://cds.cern.ch/record/381429`
[6] ATLAS Collaboration ATLAS-CONF-2012-048 `http://cds.cern.ch/record/1349309`
[7] `https://twiki.cern.ch/twiki/bin/view/AtlasPublic/EgammaTriggerPublicResults`
[8] `https://twiki.cern.ch/twiki/bin/view/AtlasPublic/JetTriggerPublicResults`
[9] Cacciari M and Salam G P 2006 *Phys. Lett.* **B641** 57–61 (*Preprint* `hep-ph/0512210`)
[10] Hristova I ATL-DAQ-PROC-2012-051 `http://cds.cern.ch/record/1485638`
[11] `https://twiki.cern.ch/twiki/bin/view/AtlasPublic/MissingEtTriggerPublicResults`
[12] ATLAS Collaboration ATLAS-CONF-2013-006 `http://cds.cern.ch/record/1510157`
[13] `https://twiki.cern.ch/twiki/bin/view/AtlasPublic/TauTriggerPublicResults`
[14] Kama S ATL-DAQ-PROC-2012-061 `http://cds.cern.ch/record/1494175`